

Performance failure simulation and characteristic analysis of marine diesel engine turbocharging and gas-exchange system under different running conditions

Yihuai Hu[†] · Meng Wang¹ · Cun Zeng² · Jiawei Jiang³

(Received May 17, 2021 ; Revised June 14, 2021 ; Accepted July 4, 2021)

Abstract: Taking a two-stroke marine diesel engine as an example, this study first builds up a thermodynamic simulation model of a turbocharging and gas-exchange system in MATLAB/Simulink, which is verified by the experimental results of a diesel engine under normal conditions. The boundary condition and corresponding model parameters are changed to simulate typical performance failures, including extremely high engine room temperature, intake filter blockage, intercooler fouling at the water side, overly high intercooler cooling water temperature, scavenging port fouling, clogged turbine nozzle, worn turbocharger bearing, and turbine exhaust passage fouling. The thermodynamic parameters of a diesel engine under different running conditions and performance failures are analyzed in terms of relative deviation, which demonstrates the relationship between the performance failures and thermodynamic parameters. This relationship could be mostly free of the engine running conditions. Finally, a normalization method is proposed to eliminate the influences of the engine room temperature and intercooler cooling water temperature. Thus, the performance failures could be detected according to the relative deviation of the proposed thermodynamic parameters under different running conditions throughout the entire engine working range. This method may provide a more practical foundation and possible breakthrough in the condition monitoring and failure diagnosis of marine diesel engines onboard ships.

Keywords: Marine diesel engine, Turbocharging and gas-exchange, Engine performance simulation, Failure diagnosis

Nomenclature

| | | | |
|--------------|--|---------------|--|
| ΔP_1 | local pressure loss at air filter inlet | T_{clin} | air temperature at intercooler inlet |
| ΔP_2 | resistance loss along air filter way | T_{clout} | air temperature at intercooler outlet |
| ρ | inlet air density | P_{clin} | air pressure at intercooler inlet |
| l | pipe length of the air filter | P_{clout} | air pressure at intercooler outlet |
| d | pipe diameter of the air filter | T_w | cooling water inlet temperature of intercooler |
| P_0 | compressor inlet pressure | ε | cooling coefficient of cooling water |
| λ | inlet air viscous coefficient | m_{c0} | rated air flow rate of intercooler |
| v | inlet air flow rate | ΔP_0 | initial air pressure loss of intercooler |
| A_r | equivalent inlet area of compressor | P_{im} | air pressure in scavenging tank |
| T_{cin} | inlet air temperature of the compressor | T_{im} | air temperature in scavenging tank |
| T_{cout} | outlet air temperature of the compressor | V_{im} | scavenging tank volume |
| n_{tc} | turbocharger rotating speed | m_d | intake air flow of engine |
| π_c | compressor pressure ratio | η_v | charging efficiency of engine |
| k | polytropic compression index | n_e | running speed of engine |
| R | gas constant | K | increase factor of exhaust gas temperature |
| | | α | excess air coefficient |

[†] Corresponding Author (ORCID: <http://orcid.org/0000-0003-3000-7855>): Professor, Department of Marine Engineering, Shanghai Maritime University, 1550 Haigang Avenue, Lingang New City, Pudong New Area, Shanghai, P. R. China, E-mail: yhhu@shmtu.edu.cn, Tel: +86-13651857174

1 M. S., Department of Marine Engineering, Shanghai Maritime University, E-mail: mengw725@foxmail.com, Tel: +86-18521012168

2 Ph. D. Candidate, Department of Marine Engineering, Shanghai Maritime University, E-mail: zc.shmtu@foxmail.com, Tel: +86-18916271125

3 Researcher, Department of Marine Engineering, Shanghai Maritime University, E-mail: oliver1992@vip.qq.com, Tel: +86-18635191739

This is an Open Access article distributed under the terms of the Creative Commons Attribution Non-Commercial License (<http://creativecommons.org/licenses/by-nc/3.0>), which permits unrestricted non-commercial use, distribution, and reproduction in any medium, provided the original work is properly cited.

| | |
|-------------|---------------------------------------|
| m_f | injected fuel quantity per cylinder |
| T_i | output torque of engine |
| T_e | exhaust gas temperature of engine |
| g_i | fuel oil consumption rate of engine |
| H_u | fuel oil low heat value |
| V_d | evacuation volume per cylinder |
| η_i | indicated working efficient of engine |
| P_{em} | gas pressure in exhaust manifold |
| T_{em} | temperature in exhaust manifold |
| m_{out} | mixed gases flow in exhaust manifold |
| V_{em} | exhaust manifold volume |
| n'_{tc} | similar rotating speed of turbine |
| T_{tout} | turbine gas outlet temperature |
| M_t | turbine output torque |
| m_t | gas flow of turbine |
| η_{ts} | turbine working efficient |
| F_{res} | gas flow area of turbine |
| π_t | turbine expansion ratio |
| μ_t | flow coefficient of turbine |
| ψ | flow function coefficient of turbine |
| η_m | turbocharger working efficiency |
| I_{tc} | turbocharger rotating inertia |
| l/d | aspect ratio of compressor filter |
| μ_s | intake air flow coefficient |
| μ_T | turbine nozzle flow coefficient |
| P_b | turbine back pressure |
| N_{C1} | compressor coefficient 1 |
| N_{C2} | compressor coefficient 2 |
| N_C | intercooler cooling coefficient |
| N_{t1} | turbine coefficient 1 |
| N_{t2} | turbine coefficient 2 |
| N_{cf} | intercooler flow coefficient |
| N_{tf} | turbine flow coefficient |

1. Introduction

With the rapid development of ship technology, ocean-going ships are tending to be large scaled and intelligent. When abnormal phenomena occur during ship operation, it becomes increasingly difficult for engineers in the engine room to quickly analyze the causes of failure and respond accurately in the face of complicated puzzling information. The development of marine engine condition monitoring and failure diagnosis technology can help engineers address failures in time, save over 30% overhaul

costs, reduce maintenance labor by 37%, and avoid accidents [1]. Additionally, the utilization of equipment can be extended, resulting in considerable economic benefits. The thermodynamic parameters of marine diesel engines, with significant failure information, have the characteristics of little external interference, good information quality, a wide diagnosis range, and strong availability, and have been the main method for the condition monitoring of modern ships. However, the main marine diesel engine of a ship is a complex system that integrates mechanical, electrical, thermal, and hydraulic features. It is composed of a fuel injection system, a chamber combustion system, a turbocharging and gas-exchange system, and starting and reversing systems [2]. There are many potential failure excitations and abundant characteristic parameters. No simple corresponding relationship exists between them, which is also influenced by the ship navigation conditions and engine operation boundary conditions [3]. The acquisition of a definite and invariable relationship between performance failures and thermodynamic parameters under different running conditions is the main bottleneck in the application of failure diagnosis to large marine diesel engines [4].

The failure simulation of a marine diesel engine by numerical calculation of the thermodynamic working process is a good way to reveal the intrinsic relationship between the thermodynamic parameters of the main engine and its performance failures under different ship navigation and engine running conditions, to solve the problem of parameter optimization, and provide training samples for automatic failure diagnosis by establishing a quantitative relationship between performance failures and characteristics under various engine operating conditions. In recent years, some scholars have carried out performance failure simulations and characteristic analyses of marine diesel engines. Jose Antonio Pagán Rubio *et al.* introduced a four-stroke high-speed marine diesel engine simulator with a one-dimensional thermodynamic engine model developed in the AVLBoost. Numerous typical failures can be simulated, and a failure database for diagnosis can be built in this way [5]. Theotokatos *et al.* employed mean value engine models based on a zero-dimensional model. The simulation accuracy was validated against experimental data from ship trials, which can be used for engine performance prediction [6]. Matulić *et al.* simulated the failure of a two-stroke low-speed marine diesel engine based on an AVL multi-zone combustion model and other models. It was verified with onboard measurements under 40%, 60%, and 100% engine load with 2%–7% inaccuracy [7]. However, the thermodynamic parameters of diesel

engines are not only related to performance failures, but also to their operating conditions, such as the engine room air temperature and cooling water inlet temperature [8]. To consider these factors, considerably more modeling should be carried out, which is nearly impossible for marine diesel engines. The acquisition of a definite and invariable relationship between thermodynamic parameters and performance failures under different running conditions is the main bottleneck in the application of failure diagnosis for large marine diesel engines, which has not been successfully solved by previous researchers.

This study considers a MAN B&W 6S35ME-B type two-stroke marine diesel engine as an example. The turbocharging and gas-exchange simulation system of the engine is built-up in MATLAB/Simulink with an average thermodynamic simulation model, which is verified by experimental results under normal conditions. The boundary condition and corresponding model parameters were changed to simulate typical performance failures. The thermodynamic parameters of a diesel engine under different working conditions and performance failures were analyzed in terms of the relative deviation, which demonstrated the relationship between the performance failures and thermodynamic parameters. This relationship could be mostly free of the engine running conditions. Finally, a normalization method is proposed to eliminate the influences of the engine room temperature and intercooler cooling water temperature. Future research will be carried out to verify this method, which lays a more practical foundation for the performance failure diagnosis of the diesel engine turbocharging and gas-exchange system.

2. Numerical Calculation Under Normal Conditions

2.1 Simulation Models

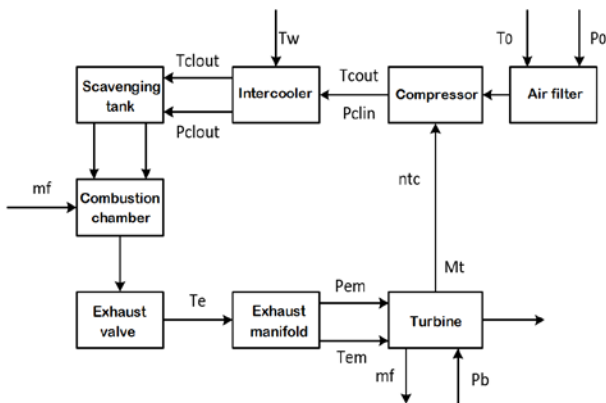


Figure 1: Module composition of diesel engine turbocharging and gas-exchange system

The simulated engine is a two-stroke marine diesel engine with a MAN TCR 22 turbocharger equipped with an emergency blower of 18.5 kW. The rated speed was 142 r/min, and the rated power was 3570 kW with a 350/1550 mm diameter/stroke. The outlet diameter of the compressor end was 290 mm, and the scavenging tank volume was 167 L. The exhaust main pipe diameter is 796 mm and the length is 604.6 mm. The maximum compression ratio of the turbo charger was 5.0. The entire diesel engine turbocharging and gas-exchange system is divided into seven subsystems: air filter, compressor, intercooler, scavenging tank, chamber combustion, exhaust valve, exhaust manifold, and turbine, as shown in Figure 1 [9]. The thermodynamic model of the diesel engine system is shown in Figure 2. The mathematical simulation models are described as follows.

1) Air Filter

It is simplified as a one-dimensional steady flow unit with main losses of local pressure drop ΔP_1 and drag loss along the way ΔP_2 [10].

$$\Delta P_1 = \frac{1}{2} \epsilon \rho v^2 \tag{1}$$

$$\Delta P_2 = \frac{1}{2} \lambda \rho \frac{l}{d} v^2 \tag{2}$$

$$\Delta P_0 = \Delta P_1 + \Delta P_2 \tag{3}$$

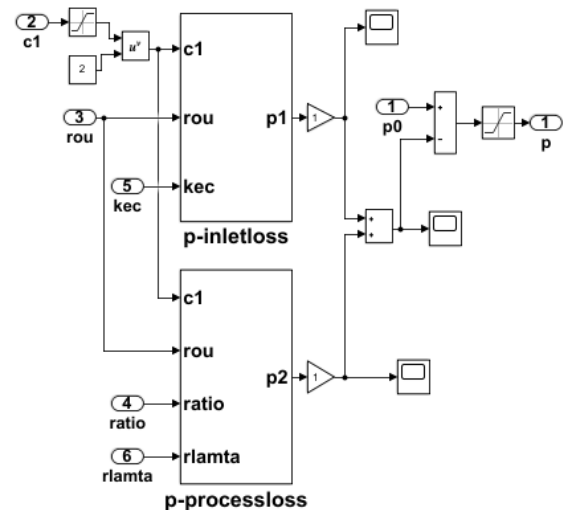


Figure 3: Simulation model of air filter in Matlab/Simulink

Where $\Delta P_1, \Delta P_2, \rho, l, d, P_0$ are local pressure loss at the inlet, resistance loss along the way, air density, pipe length, pipe diameter and compressor inlet pressure respectively. The loss coefficient ϵ is 0.5; The air viscous coefficient is taken as $\lambda =$

0.00001983 pa · s. Air flow rate is $v = m_c / (\rho A_r)$, obtained from the compressor mass flow rate. Inlet equivalent area of compressor A_r is 0.039. The air filter simulation model in Matlab/Simulink is shown in **Figure 3**.

2) Compressor

According to a one-dimensional adiabatic compression model with a compressor characteristic curve, the outlet temperature of the compressor [11]

$$T_{c_{out}} = T_{c_{in}} \left\{ 1 + \left[(\pi_c)^{\frac{k-1}{k}} - 1 \right] \frac{1}{\eta_{cs}} \right\} \quad (4)$$

The obtained torque of the compressor is

$$M_C = 30 \dot{m}_c k R T_{c_{in}} \left[\pi_c^{\frac{k-1}{k}} - 1 \right] / [\pi \eta_{cs} n_{tc} (k - 1)] \quad (5)$$

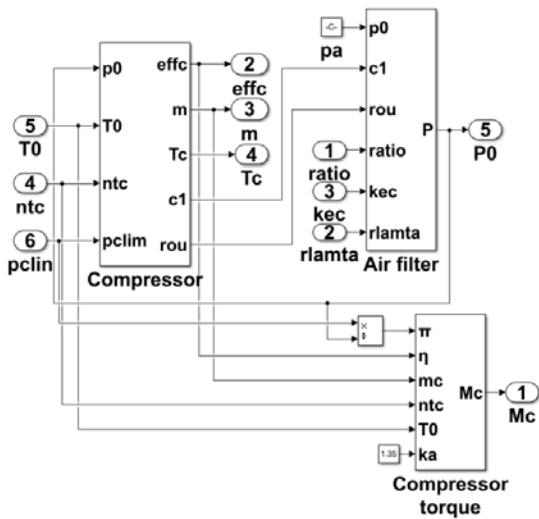


Figure 4: Simulation model of air compressor in Matlab/Simulink

where T_{cin} and T_{cout} are the inlet and outlet temperatures of the compressor, respectively. n_{tc} and π_c are the supercharger speed and compressor pressure ratio respectively. Here, $\pi_c = P_{clin}/P_0$, and η_{cs} and \dot{m}_c are the adiabatic efficiency and air flow rate of the compressor, respectively. The polytropic compression index and gas constant k and R can be obtained with imported n_{tc} and π_c . The simulation model of the compressor in the MATLAB/Simulink is shown in **Figure 4**.

3) Intercooler

Owing to its high heat exchange efficiency, the thermal inertia of the intercooler can be generally ignored, and only the cooling

effect and pressure loss are considered, which are treated as a throttle cooling and pressure dropping unit [12]. With the cooling coefficient ε , the outlet temperature of the intercooler is

$$T_{clout} = T_{clin} + \varepsilon(T_{wi} - T_{clin}) \quad (6)$$

The pressure drop of the intercooler is related to the air flow rate, and the outlet air pressure of the intercooler can be expressed as [12]

$$P_{clout} = P_{clin} - \Delta P_0 (\dot{m}_c / \dot{m}_{c0}) \quad (7)$$

where, T_{clin} , T_{clout} , and P_{clin} , P_{clout} are the air temperature and pressure at the intercooler inlet and outlet, respectively. T_w is the cooling water inlet temperature of the intercooler, ε is its cooling coefficient, and \dot{m}_{c0} is the rated air flow rate of the intercooler. The initial air pressure loss of the intercooler P_0 is 400 Pa [13]. The simulation model of the intercooler in MATLAB/Simulink is shown in **Figure 5**.

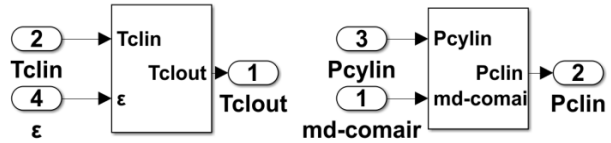


Figure 5: Simulation model of inter-cooler in Matlab/Simulink

4) Scavenging Tank

The scavenging tank is modeled using the volumetric method calculated by the energy, mass, and ideal gas law conservation equations. The air pressure in the scavenging tank is [14]

$$P_{im} = kR(\dot{m}_c T_{clout} - \dot{m}_d T_{im}) / V_{im} \quad (8)$$

The outlet air temperature in the scavenging tank is obtained from the ideal gas law equation as

$$T_{im} = P_{im} V_{im} / m_g R_g \quad (9)$$

where, P_{im} and T_{im} are the air pressure rate and temperature in the scavenging tank, respectively. Here, the scavenging tank volume V_{im} of the MAN B&W 6S35ME-B9 diesel engine was calculated to be 0.167 m³. m_d is the intake airflow of the engine. The scavenging tank simulation model in MATLAB/Simulink is shown in **Figure 6**.

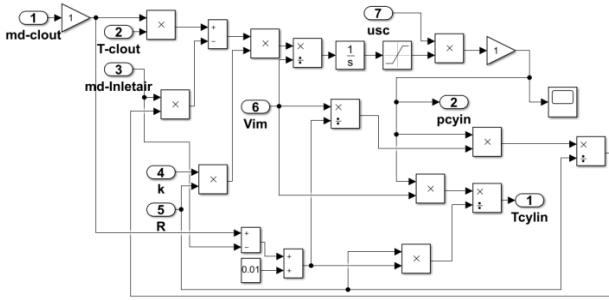


Figure 6: Simulation model of scavenging tank in Matlab/Simulink

5) Chamber Combustion

The intake air flow of a diesel engine is obtained from the theoretical airflow of the engine with a filled cylinder

$$\dot{m}_d = \eta_v P_{im} V_d n_e \phi / 60 R T_{im} \tag{10}$$

where η_v is the charging efficiency of the engine, which is generally regarded as a single function of the running speed n_e of the diesel engine. Here, $\eta_v = a_2 * n_e^2 + a_1 * n_e + a_0$, here $a_2 = -5.363 * 10^{-7}$, $a_1 = 2.04 * 10^{-3}$, $a_0 = 0.576107$.

The exhaust gas temperature in the exhaust branch is expressed as

$$T_e = T_{im} + K / (1 + L_0 \alpha) \tag{11}$$

where, K and α are the increase factors of the exhaust gas temperature and excess air coefficient, respectively. The required air per fuel L_0 is 14.3. The exhaust gas temperature rise factor K is a function of the air-fuel ratio [13], which is interpolated with the excess air coefficient. In MATLAB/Simulink, the simulation model of the exhaust branch temperature of the diesel engine is shown in **Figure 7**.

Output torque of diesel engine

$$T_i = \frac{30 P_i}{\pi n_e} = \frac{30 \eta_i H_u \dot{m}_f}{\pi n_e} \tag{12}$$

Its fuel oil consumption

$$g_i = \frac{3600 \dot{m}_f}{P_e} = \frac{3600}{\eta_i H_u \dot{m}_f} \tag{13}$$

Where \dot{m}_f, T_i, T_e, g_i are the fuel injection quantity per cylinder, output torque, exhaust gas temperature and fuel oil consumption rate of the diesel engine respectively. The lower fuel heat value

H_u is $42700 \text{ kJ}/(\frac{\text{kg}}{\text{K}})$. The evacuation volume per cylinder V_d is 0.87 m^3 . η_i is the indicated working efficiency of engine. The combustion dynamics and thermodynamic simulation model of combustion in the cylinder in Matlab/Simulink is shown in **Figure 8**.

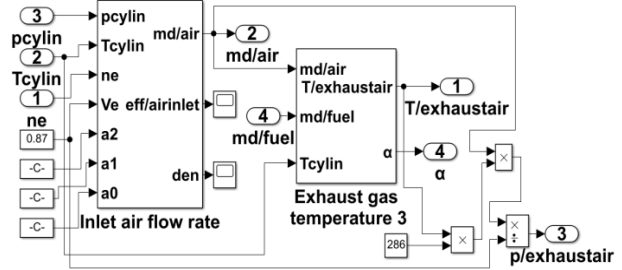


Figure 7: Simulation model of exhaust branch in Matlab/Simulink

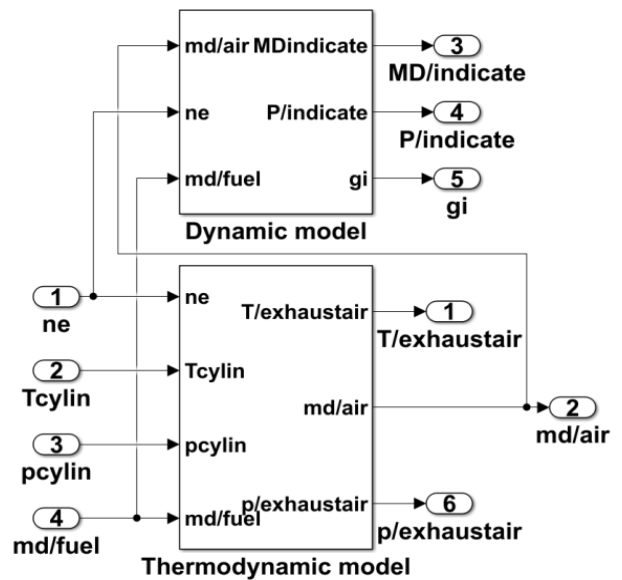


Figure 8: Thermodynamic simulation model of combustion in Matlab/Simulink

6) Exhaust Manifold

The exhaust gas in the manifold is also modeled with the "Volumetric method" and exhaust gas pressure

$$P_{em} \dot{V} = k_e R_e (m_{out} \dot{T}_e - \dot{m}_t T_{em}) / V_{em} \tag{14}$$

The gas temperature in the exhaust manifold is obtained from the ideal gas equation law

$$T_{em} = P_{em} V_{em} / m_{em} R_e \tag{15}$$

where P_{em}' and T_{em} are the gas pressure rate and temperature in the exhaust manifold, respectively. Here, the mixed gases in the exhaust manifold m_{out} are $m_a + m_f$, and the exhaust pipe volume V_{em} is 0.3 m³. The exhaust manifold simulation model in MATLAB/Simulink is shown in **Figure 9**.

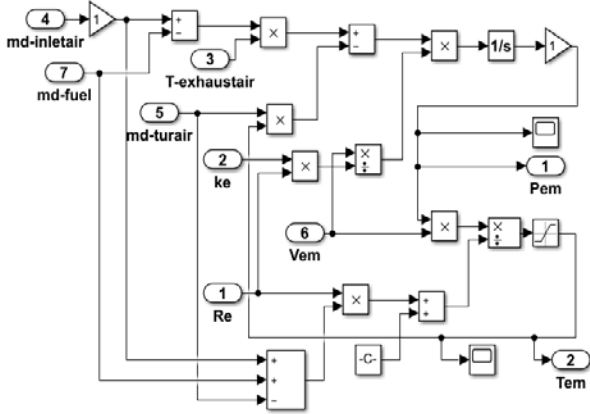


Figure 9: Simulation model of exhaust manifold in Matlab/Simulink

7) Gas Turbine

The turbine efficiency is fitted by the embedded RBF function in MATLAB by adopting the s-function from the turbine characteristic curve [14].

$$n_{tc}' = \frac{n_{tc}}{\sqrt{T_{em}}} \quad (16)$$

The turbine outlet temperature is

$$T_{tout} = T_{em} [1 - \eta_{ts} (1 - \pi_t^{\frac{1-k_t}{k_t}})] \quad (17)$$

The turbine output torque is

$$M_t = 30 \dot{m}_t \eta_{ts} k_t R T_{em} (1 - \pi_t^{\frac{1-k_t}{k_t}}) / \pi n_{tc} (k_t - 1) \quad (18)$$

The turbine is equivalent to a throttle nozzle for a simplified calculation. The gas flow, \dot{m}_t , is obtained as a one-dimensional isentropic expansion process:

$$\dot{m}_t = \mu_T F_{res} \psi P_{em} / \sqrt{R T_{em}} \quad (19)$$

When $\pi_t < \left(\frac{k_t+1}{2}\right)^{\frac{k_t}{k_t-1}}$:

$$\psi = \sqrt{\frac{2k_t}{k_t-1} \left[\pi_t^{\frac{2}{k_t}} - \pi_t^{\frac{1+k_t}{k_t}} \right]} \quad (20)$$

When $\pi_t \geq \left(\frac{k_t+1}{2}\right)^{\frac{k_t}{k_t-1}}$:

$$\psi = \left(\frac{2}{k_t+1}\right)^{\frac{k_t}{k_t+1}} \sqrt{\frac{2k_t}{k_t+1}} \quad (21)$$

where, T_{tout} , M_t , \dot{m}_t , η_{ts} , and F_{res} (A0 in the following figure) are the gas outlet temperature, turbine output torque, gas flow, turbine efficiency, and gas flow area, respectively. The turbine expansion ratio π_t was P_{em}/P_b . ψ, μ_T are the flow function and flow coefficient, respectively, where F_{res} is 0.039 and μ_T is 0.7. The turbine simulation model in MATLAB/Simulink is shown in **Figure 10**.

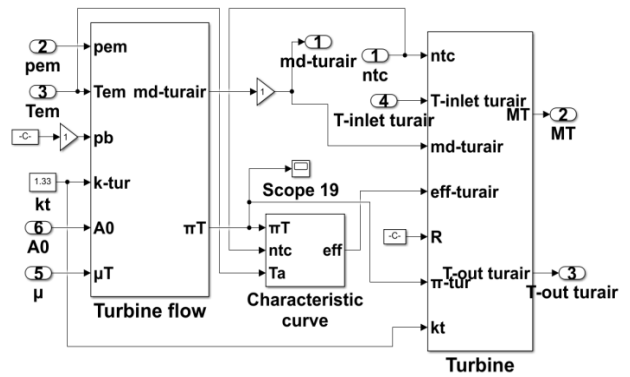


Figure 10: Simulation model of turbine in Matlab/Simulink

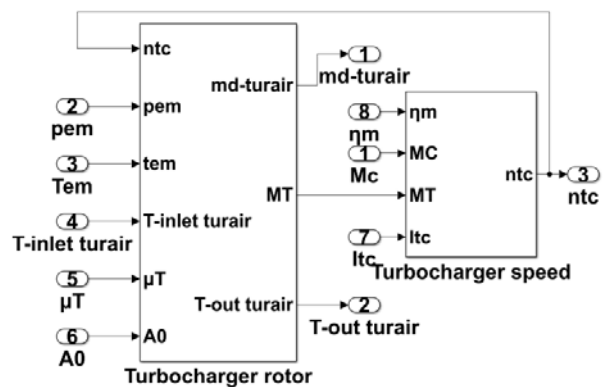


Figure 11: Simulation model of rotor in Matlab/Simulink

The turbocharger rotating speed can be obtained from the D'Alembert's principle as

$$n_{tc}' = 30(\eta_m M_T - M_c) / \pi I_{tc} \quad (22)$$

where, η_m and I_{tc} are the turbocharger mechanical working efficiency and turbocharger rotating inertia, respectively, where η_m is 0.89 and I_{tc} is 16. The turbine rotor simulation model in MATLAB/Simulink is shown in **Figure 11**.

Table 1: Comparison between experimental and simulated results

| Thermodynamic Parameters | Data Type | Engine Load | | | |
|--|-------------|-------------|------------|------------|------------|
| | | 25% | 50% | 75% | 90% |
| Engine Speed n_e (r/min) | Measured | 89 | 114 | 129 | 140 |
| Injected Fuel Quantity m_f (g) | Measured | 6.11 | 8.49 | 10.28 5 | 12.58 |
| Turbocharger Speed n_{tc} (r/min) | Measured | 9679 | 14961 | 18300 | 19135 |
| | Calculation | 9985 | 14890 | 18030 | 19370 |
| Turbine Outlet Gas Temperature T_{out} (K) | Measured | 540.7 | 541.1 | 523.6 | 542.0 |
| | Calculation | 563.2 | 532.0 | 490.8 | 536.4 |
| Turbine Inlet Gas Temperature T_{em} (K) | Measured | 590.7 | 636.4 | 649.0 | 685.3 |
| | Calculation | 602.7 | 612.1 | 619.3 | 700.6 |
| Exhaust Gas Temperature T_e (K) | Measured | 592.0 3 | 635.4 7 | 601.1 3 | 675.9 |
| | Calculation | 581.2 | 624.2 | 604.0 | 671.4 |
| Compressor Inlet air Temperature T_{im} (K) | Measured | 313.4 6 | 315.5 3 | 317.7 4 | 320.8 2 |
| | Calculation | 315.9 | 319.1 | 323.2 | 325.8 |
| Compressor air Outlet Temperature T_{cout} (K) | Measured | 339.3 25 | 399.9 1 | 447.5 6 | 469.5 6 |
| | Calculation | 342.8 | 396.2 | 443.8 | 474.5 |
| Scavenging Air Pressure P_{im} (kpa) | Measured | 144 | 211 | 270 | 300 |
| | Calculation | 153.2 | 229.4 | 305.2 | 340.3 |
| Fuel Consumption Rate g_i (kg/kw-h) | Measured | 218.6 | 221.3 | 199.1 | 192.4 |
| | Calculation | 209.9 | 207.4 | 196.1 | 194.8 |

2.2 Simulation Results

Thermodynamic parameters such as the running speed, power, and intake air temperature of the diesel engine were recorded in an engine laboratory at 25%, 50%, 75%, and 90% engine

operation conditions. A comparison between the experimental and simulated results is presented in **Table 1**.

It is verified that the errors of most measured and calculated parameters are within 5%, except for a few parameters. These results indicate that the simulation models of the diesel engine turbocharging and gas-exchange system in MATLAB/Simulink are feasible, and the thermodynamic parameters from the diesel engine simulation calculation, such as the temperature, pressure, speed, and fuel consumption rate, can reflect the condition of the engine under different operating conditions.

3. Simulation and Analysis of Performance Failures

3.1 Performance Failure Simulation

Based on the diesel engine simulation model mentioned above, some performance failures of the super-charging and gas-exchange system were simulated by changing the model parameters to reveal the variation rules of each thermal parameter under different failure conditions. Additionally, the variation in the boundary conditions of a diesel engine also affect its operating performance and thermal parameters, such as the compressor intake air temperature and intercooler cooling water inlet temperature. For ease of representation, these are collectively referred to as performance failures; the performance failures for some failure states and the setting of the model parameters are listed in **Table 2**.

In addition to the conventional thermodynamic parameters, some combined parameters are proposed here to indicate the performance failure of diesel engine, including the compressor

Table 2: Performance failures and modeling parameters

| Performance Failure | Modelling Parameter | Normal Status | Failure Status 1 | Failure Status 2 | Failure Status 3 | Failure Status 4 | Failure Status 5 |
|--|--|---------------|------------------|------------------|------------------|------------------|------------------|
| Too High Engine Room Temperature | Ambient Temperature T_{cin} (K) | 286 | 300 | 315 | 329 | 343 | 357 |
| Intake Filter Blockage | Aspect Ratio l/d | 3 | 300 | 600 | 900 | 1200 | 1500 |
| Intercooler Fouling at Water Side | Cooling Coefficient of Intercooler ε | 0.89 | 0.85 | 0.80 | 0.75 | 0.70 | 0.65 |
| Too High Intercooler Cooling Water Temperature | Cooling Water Temperature T_w (K) | 300 | 315 | 330 | 345 | 360 | 375 |
| Scavenging Port Fouling | Intake Air Flow Coefficient u_ζ | 0.40 | 0.38 | 0.36 | 0.34 | 0.32 | 0.30 |
| Clogged Turbine Nozzle | Turbine nozzle Flow Coefficient u_T | 0.70 | 0.67 | 0.63 | 0.61 | 0.58 | 0.55 |
| Worn Turbocharger Bearing | Working Efficiency of Turbocharger η_m | 0.89 | 0.85 | 0.80 | 0.75 | 0.70 | 0.65 |
| Turbine Exhaust Passage Fouling | Turbine Back Pressure P_b (Pa) | 111400 | 116970 | 122540 | 128110 | 133680 | 139250 |

coefficient N_{c1} , turbine coefficient N_{t1} , compressor coefficient N_{c2} , turbine coefficient N_{t2} , intercooler cooling coefficient N_c , intercooler flow coefficient N_{cf} , and turbine flow coefficient N_{tf} .

$$N_{c1} = \frac{(T_{c_{out}} - T_{c_{in}})P_{c_{clin}}}{n_{tc}} \quad (23)$$

$$N_{t1} = \frac{n_{tc}}{(T_{em} - T_{t_{out}})P_{em}} \quad (24)$$

$$N_{c2} = \frac{P_{c_{clin}}}{n_{tc}} \quad (25)$$

$$N_{t2} = \frac{n_{tc}}{T_{em}} \quad (26)$$

$$N_c = \frac{(T_{c_{clin}} - T_{c_{tout}})}{(T_{c_{clin}} - T_{win})} \quad (27)$$

$$N_{cf} = P_{c_{clin}} - P_{c_{tout}} \quad (28)$$

$$N_{tf} = P_{em} - P_b \quad (29)$$

These thermodynamic parameters are represented in terms of the relative deviation under different running conditions and performance failures [15].

$$\varepsilon = \frac{x - x_0}{x_0} \quad (30)$$

where x and x_0 are the thermodynamic parameters of the diesel engine model under failure and normal conditions, respectively.

3.2 Performance Failures Analysis

The simulated results of turbocharging and gas-exchanging systems under different running conditions and various performance failures were analyzed using 18 thermodynamic parameters, as shown in the following figures. The 18 calculated thermodynamic parameters are represented by different numbers, as listed in **Table 3**.

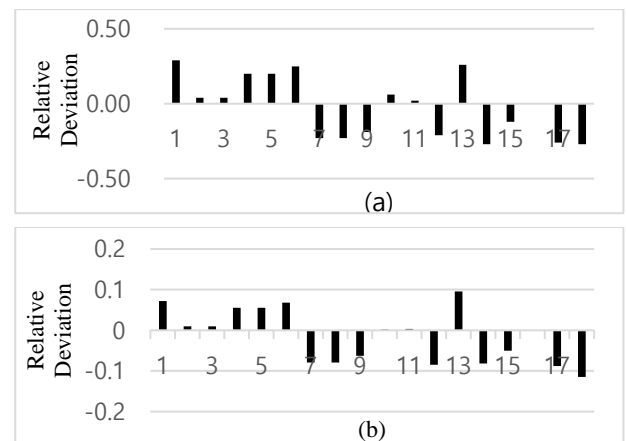
Table 3: Thermodynamic parameters represented with numbers

| Number | Parameter | Parameter Description |
|--------|----------------|--------------------------------------|
| 1 | $T_{c_{out}}$ | Outlet Air Temperature of Compressor |
| 2 | $T_{c_{lout}}$ | Intercooler Outlet Air Temperature |
| 3 | T_{im} | Scavenger Air Temperature |
| 4 | T_e | Exhaust Gas Temperature |
| 5 | T_{em} | Exhaust Gas Temperature in Manifold |
| 6 | $T_{t_{out}}$ | Turbine Outlet Gas Temperature |
| 7 | $P_{c_{clin}}$ | Intercooler Inlet Air Pressure |

| | | |
|----|----------|----------------------------------|
| 8 | P_{im} | Intercooler Outlet Air Pressure |
| 9 | P_{em} | Exhaust Gas Pressure in Manifold |
| 10 | n_{tc} | Turbocharger Rotating Speed |
| 11 | g_e | Engine Fuel Oil Consumption Rate |
| 12 | N_{c1} | Compressor Coefficient |
| 13 | N_{t1} | Turbine Coefficient |
| 14 | N_{c2} | Compressor Coefficient |
| 15 | N_{t2} | Turbine Coefficient |
| 16 | N_c | Intercooler Cooling Coefficient |
| 17 | N_{cf} | Intercooler Flow Coefficient |
| 18 | N_{tf} | Turbine Flow Coefficient |

1) Extremely High Inlet Air Temperature

Owing to the different shipping routes, the influence of the engine room temperature cannot be ignored, and the engine inlet air temperature could be different. The relative deviations of the thermodynamic parameters under different running speeds and engine room temperatures are shown in **Figure 12**. It can be observed that when the engine room temperature rises, the decrease in inlet air density worsens the chamber combustion inside the cylinder. The exhaust air temperature T_e , exhaust gas temperature in manifold T_{em} , and turbine outlet gas temperature $T_{t_{out}}$ of the diesel engine increase significantly, whereas the intercooler inlet air pressure $P_{c_{clin}}$, air pressure in the scavenging tank P_{im} , and exhaust air pressure in the manifold P_{em} decrease. The most obvious change was the rise in the compressor outlet air temperature $T_{c_{out}}$. With respect to the combined parameters, the turbine coefficient N_{t1} increases the most obviously, whereas the compressor coefficient N_{c1} , compressor coefficient N_{c2} , turbine coefficient N_{t2} , intercooler flow coefficient N_{cf} , and turbine flow coefficient N_{tf} all decrease to varying degrees.



Thermodynamic Parameters

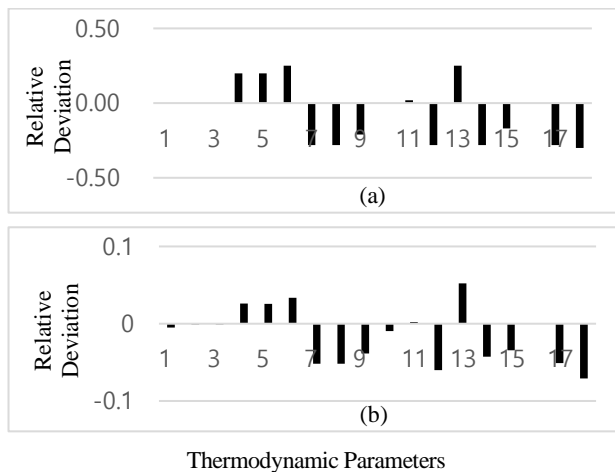
(a) The speed is 129 r/min and engine room temperature of 400 K
 (b) The speed is 116 r/min and engine room temperature of 315 K

Figure 12: Relative deviation under different engine room temperatures and running speeds

Comparing **Figure 12 (a)** and **Figure 12 (b)**, it can be observed that the variations in the various parameters under different running conditions are quite similar. This indicates that the performance failure behavior of characteristic parameters in terms of the relative deviation is quite clear and immovable, even under different running conditions of the diesel engine, which is greatly convenient for failure diagnosis.

2) Intake Air Room Filter Blockage

The pressure drop due to resistance along the way of the filter mesh was simulated by changing the length diameter ratio of the filter (l/d) in **Equation (2)** to simulate the blockage of the air filter in the diesel engine.



(a) l/d is 1500 and the speed is 129 r/min
 (b) l/d is 300 and the speed is 116 r/min

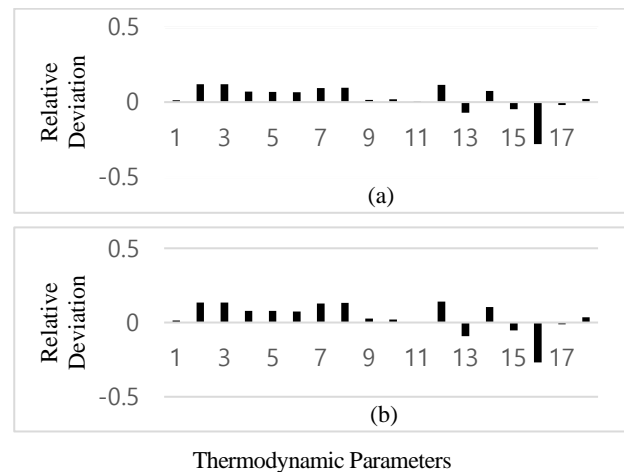
Figure 13: Relative deviation under different air filter l/d and running speeds

Figure 13 shows the relative deviation of the characteristic parameters of the diesel engine when l/d is 1500 and 300 at different running speeds. It can be observed that when the air filter is blocked, the inlet air pressure of the intercooler P_{clin} , outlet air pressure of the intercooler P_{clout} , and exhaust gas pressure in manifold P_{em} decrease, whereas the exhaust gas temperature T_e , exhaust gas temperature in the manifold T_{em} , and turbine outlet gas temperature T_{out} of the diesel engine increase, and the outlet air temperature of the compressor T_{cout} , intercooler outlet air temperature T_{clout} , and scavenger air temperature T_{im} do not change significantly. Additionally, the compressor coefficient N_{c2} , turbine coefficient N_{t2} , intercooler flow coefficient N_{cf} , and turbine flow coefficient N_{tf} decrease significantly. It was found that

when the air filter is blocked, the most affected characteristic parameter is the inlet pressure of the compressor, resulting in insufficient air into the compressor and poor combustion inside the cylinder; thus, the exhaust gas temperature increases in the exhaust manifold.

3) Intercooler Fouling at Water Side

The fouling in the intercooler water passage also has a direct impact on the intake air of diesel engines.



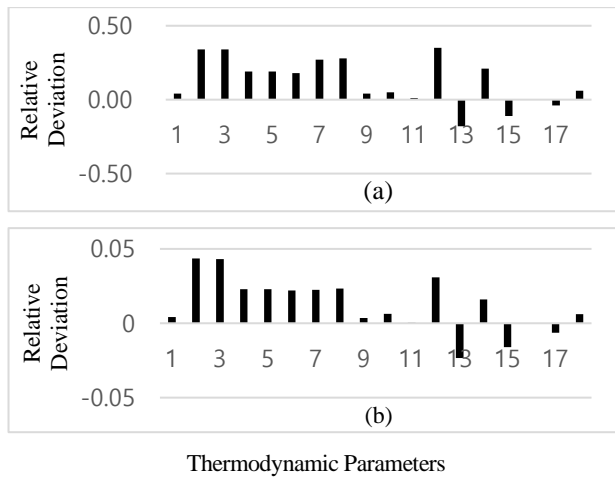
(a) The speed is 137 r/min and the cooling coefficient is 0.69
 (b) The speed is 140 r/min and the cooling coefficient is 0.65

Figure 14: Relative deviation under different intercooler cooling coefficients and running speeds

As shown in **Figure 14**, owing to the fouling on the water side of the intercooler, the cooling coefficient decreases, and it is difficult for air to exchange heat with the cooling water. The intercooler outlet air temperature T_{clout} , scavenging air temperature T_{im} , exhaust gas temperature T_e , exhaust gas temperature in manifold T_{em} , turbine outlet gas temperature T_{out} , intercooler inlet air pressure P_{clin} , and air pressure in scavenging tank P_{im} all increase significantly. The compressor coefficient N_{c1} and compressor coefficient N_{c2} increase significantly, whereas the turbine coefficients N_{t1} , N_{t2} , and N_t decrease. The turbocharger speed increases slightly, which is similar to that of the extremely high intercooler cooling water temperature described below. Here, the intercooler cooling coefficient N_c decreases significantly, whereas it remains unchanged under other failures. Therefore, the intercooler cooling coefficient N_t could be used as a unique characteristic parameter for the intercooler water fouling failure at both the air and water sides.

4) Extremely High Intercooler Cooling Water Temperature

The intercooler has a direct impact on the intake air temperature of the diesel engine, especially on the intake air temperature of the cylinder. When the intercooler inlet cooling water temperature increases, the intake air flow slightly decreases, leading to an increase in the compressor outlet air temperature $T_{c_{out}}$, intercooler outlet air temperature $T_{c_{out}}$, scavenging air temperature T_{im} , exhaust gas temperature T_e , exhaust gas temperature in manifold T_{em} , turbine outlet gas temperature T_{out} , intercooler inlet air pressure P_{clin} , and scavenging air pressure P_{im} . The compressor coefficient N_{c1} and compressor coefficient N_{c2} increase significantly, whereas the turbine coefficient N_{t1} , turbine coefficient N_{t2} , and intercooler flow coefficient N_{cf} decrease, and the turbocharger rotating speed increases slightly, as shown in **Figure 15**.



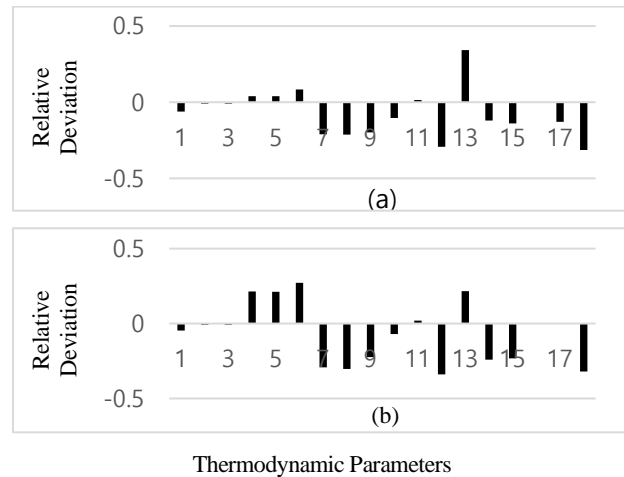
(a) The speed is 129 r/min and the inlet temperature of the cooling water is 300 K
 (b) The speed is 114 r/min and the inlet temperature of cooling water is 315 K

Figure 15: Relative deviation under different intercooler cooling water temperatures and running speeds

5) Scavenging Port Fouling

With the blockage of the scavenging port, the intake air flow into the cylinder decreases significantly, which worsens the fuel combustion inside the cylinder. The exhaust gas temperature T_e , exhaust gas temperature in the manifold T_{em} , and turbine outlet gas temperature T_{out} increase significantly, whereas the intercooler inlet air pressure P_{clin} , scavenging air pressure P_{im} , and exhaust gas pressure in the manifold P_{em} decrease. The most obvious increase is the compressor outlet air temperature $T_{c_{out}}$, as shown in **Figure 16**. The turbine coefficient N_{t1} increases most

obviously, whereas the compressor coefficients N_{c1} , N_{c2} , N_{t2} , N_{cf} , and N_{if} all decrease to varying degrees. The characteristic behavior is similar to that of air filter fouling, turbocharger bearing wear, and high inlet air temperature.



(a) The speed is 119 r/min and discharge coefficient is 0.36
 (b) The speed is 126 r/min and discharge coefficient is 0.28

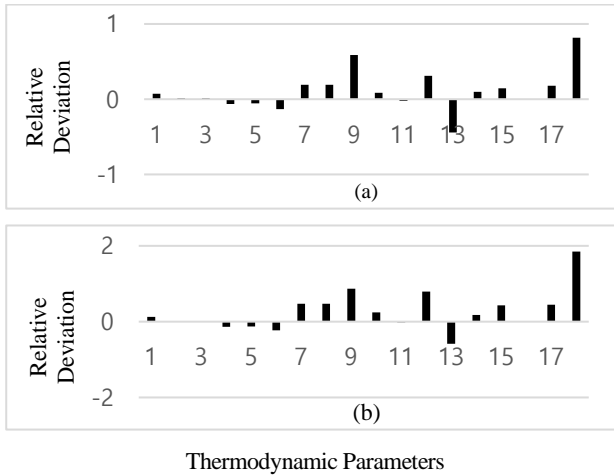
Figure 16: Relative deviation under different scavenging port flowing coefficients and running speeds

6) Turbine Nozzle Blockage

Blocked turbine nozzles can block gas flow into the turbine, which significantly increases the exhaust gas pressure in the manifold P_{em} , whereas the exhaust temperature T_e of the diesel engine, exhaust manifold temperature T_{em} , and turbine outlet temperature T_{out} slightly decrease. When the turbine nozzle is blocked, its most direct influence is on the exhaust gas pressure in the manifold P_{em} and turbine flow coefficient N_{if} , which could be used as two characteristic parameters for turbine nozzle blockage failure, as shown in **Figure 17**.

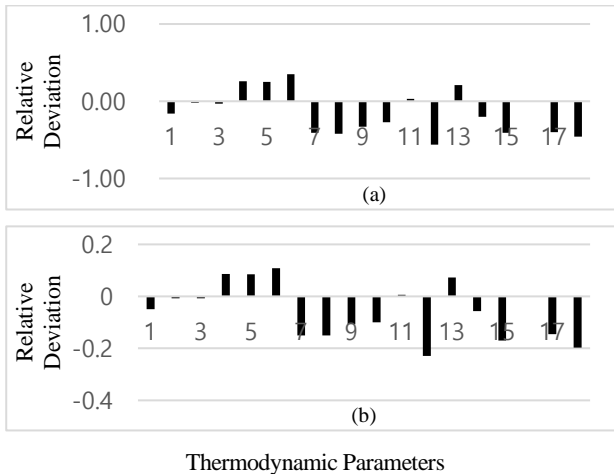
7) Worn Turbocharger Bearing

When the turbine rotor is mechanically worn out, its compressor air compression capacity and compressor air flow decrease, which cause an increase in the exhaust temperature T_e , exhaust gas temperature in manifold T_{em} , and turbine outlet gas temperature T_{out} , whereas the inlet air pressure P_{clin} , scavenging air pressure P_{im} , exhaust gas pressure in the manifold P_{em} , and turbocharger rotating speed n_{tc} decrease significantly, similar to the case in the turbine outlet passage fouling failure, as shown in **Figure 18 and 19**.



Thermodynamic Parameters
 (a) The speed is 132 r/min and flow coefficient is 0.35
 (b) The speed is 110 r/min and flow coefficient is 0.35

Figure 17: Relative deviation under different nozzle flowing coefficients and running speeds



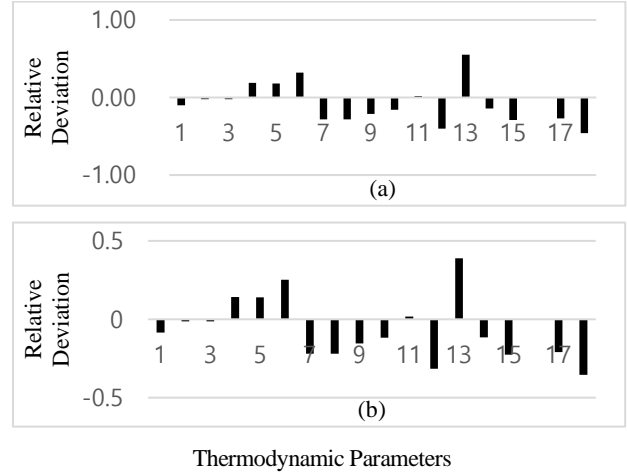
Thermodynamic Parameters
 (a) The speed is 129 r/min and mechanical efficiency is 0.445
 (b) The speed is 118 r/min and mechanical efficiency is 0.668

Figure 18: Relative deviation under different turbocharger mechanical efficiencies and running speeds

8) Turbine Outlet Passage Fouling

The turbine outlet passage fouling was simulated by increasing the back pressure during simulation. As shown in **Figure 19**, a higher back pressure of the turbine causes an increase in the exhaust gas temperature T_e , exhaust gas temperature in manifold T_{em} , and turbine outlet gas temperature T_{out} . The most direct impact is the decrease in the turbine working capacity, which reduces the turbocharger speed n_{tc} , intercooler inlet air pressure P_{clin} , intercooler outlet air pressure P_{clout} , scavenging air pressure P_{im} , and exhaust gas pressure in manifold P_{em} . With respect to the combined parameters, the increase in the turbine coefficient N_{t1}

is the most obvious, whereas the compressor coefficient N_{c1} , compressor coefficient N_{c2} , turbine coefficient N_{t2} , intercooler flow coefficient N_{cf} , and turbine flow coefficient N_{tf} all decrease to some extent.



Thermodynamic Parameters
 (a) The speed is 129 r/min and the exhaust back pressure is 155960 pa
 (b) The speed is 135 r/min and the exhaust back pressure is 155960 pa

Figure 19: Relative deviation under different turbine exhaust back pressures and running speeds

In conclusion, the characteristic parameters of extremely high inlet air temperature, intake air filter blockage, scavenging port fouling, worn turbocharger bearing, and turbine outlet passage fouling exhibit similar behavior even under different operating conditions of the diesel engine. However, when the engine room temperature is extremely high, the compressor outlet temperature T_{cout} increases significantly but decreases to a certain extent in the other failures, which provides a distinguishing parameter from other failures. The engine room temperature can be measured directly, the blocked air filter can be monitored with the differential pressure of the intake air filter, and the turbine back pressure can also be measured directly at the turbine outlet. Additionally, the worn turbocharger bearing can be judged from its vibration and scavenging port fouling can be detected by the pressure difference between the intercooler outlet air and scavenging air; thus, these different failures can be identified. The characteristic parameter behavior of the extremely high intercooler cooling water temperature is considerably similar to that of intercooler fouling at the water side, but the fouled intercooler can be determined directly by the intercooler cooling coefficient N_c , and the cooling water temperature in the intercooler can be

measured directly. These two failures were the most easily distinguished. The most obvious characteristic of the turbine nozzle blockage is the obvious increase in the exhaust gas pressure in manifold P_{em} and turbine flow coefficient N_{tf} , which is not found in the other failures. In other words, the performance failure diagnosis of diesel engine turbocharging and gas-exchanging systems can be eventually realized with some other parameters and information.

4. Normalization of Parameters

In fact, extremely high inlet air temperatures and intercooler cooling water temperatures are not engine performance failures, but are different working boundary conditions, which change the thermodynamic parameters of the engine. Therefore, before performance failure diagnosis, the normalization of the engine boundary conditions should first be carried out to eliminate the influence of the different conditions. **Figures 20 and 21** show the changing trends of the 18 characteristic parameters when the engine room temperature increases from 286 K to 400 K and the intercooler cooling water temperature increases from 315 K to 420 K at engine speeds of 129 r/min and 75% load, respectively.

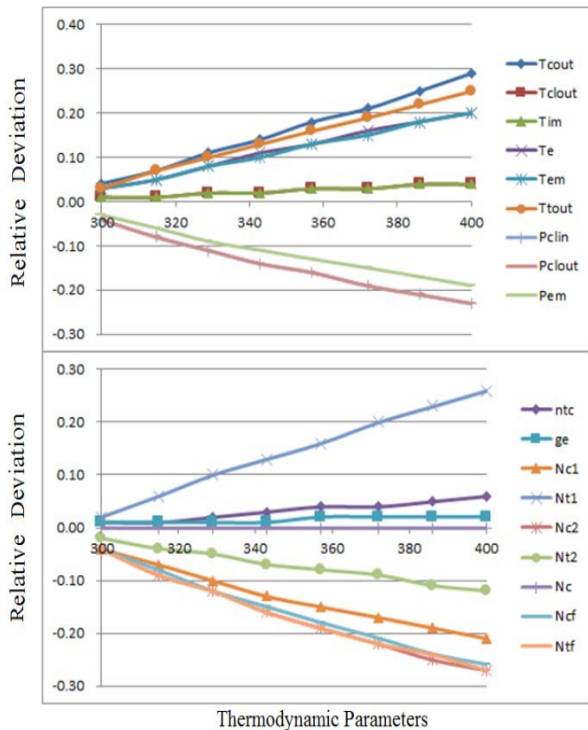


Figure 20: Relative deviations under different engine room temperatures

The same method can also be used to eliminate the influence of the intercooler cooling water temperature.

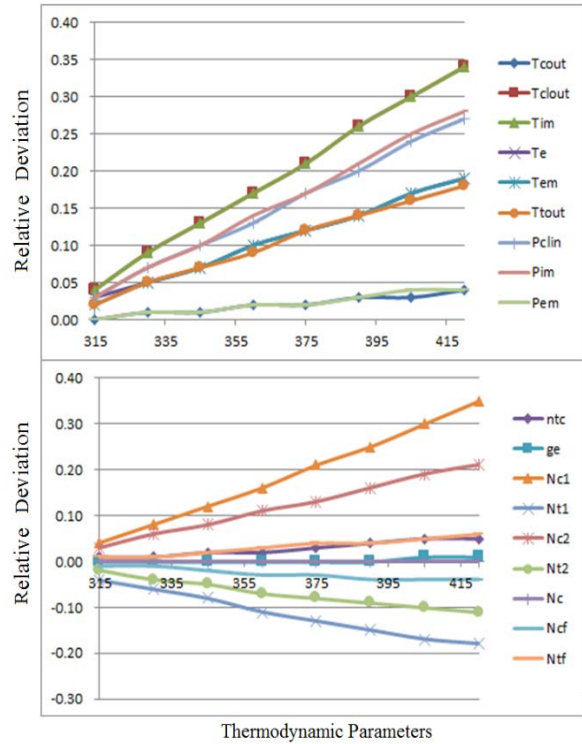


Figure 21: Relative deviations under different intercooler cooling water temperatures

It can be observed that the relative deviations of these parameters change linearly with the change in the engine room temperature and intercooler cooling water temperature. If the 286 K engine room temperature and 300 K intercooler cooling water temperature are set as the reference boundary conditions, the thermodynamic parameters under different conditions are normalized to the reference condition according to the actual engine room temperature and intercooler cooling water temperature. The relative deviation analysis and failure diagnosis of the characteristic parameters can be carried out. The specific method uses the Newton interpolation formula to calculate the relative deviation value ε at the actual temperature of a certain engine compartment at $z^\circ\text{K}$. According to **Equation (32)**, the thermal parameter x is calculated after normalizing to the reference running condition x' .

Assuming the actual engine room temperature is $z^\circ\text{K}$, the relative deviation ε of a thermodynamic parameter x could be normalized between 286 K and 400 K using the Newton interpolation method.

$$\varepsilon' = (z - 286) \frac{\varepsilon}{114} \tag{31}$$

Normalized thermodynamic parameter

$$x' = \frac{x}{1+\varepsilon'} \quad (32)$$

Subsequently, the normalized parameter x' can be compared to the parameter under the engine normal condition x_0 to obtain the relative deviation necessary for failure diagnosis.

Although the characteristic parameters have similar behaviors under different running conditions for these failures, the deviation amplitudes are quite different, as shown in **Figures 12-19**. Therefore, before the performance failure diagnosis, it is necessary to normalize the relative deviation to eliminate the influence of different running conditions before failure diagnosis. All the 18 relative deviations under different running conditions will be unified to a 1.0 maximum scale. Suppose the maximum relative deviation among the 18 relative deviation values is ε_1 , which is normalized to 1.0- or -1.0, and the other relative deviation ε_0 is normalized as ε :

$$\varepsilon = \varepsilon_0 \frac{1.0}{\varepsilon_1} \quad (33)$$

Taking the intake air filter blockage as an example, as shown in **Figure13**, the relative deviations under the two running conditions are quite different and cannot be used directly for failure diagnosis. After normalization, the two sets of parameters have nearly the same scale and are comparable. In this way, the performance failures could be identified under any engine running condition with different failure severities. The severity of the failure can be directly determined using the relative deviation scale before normalization.

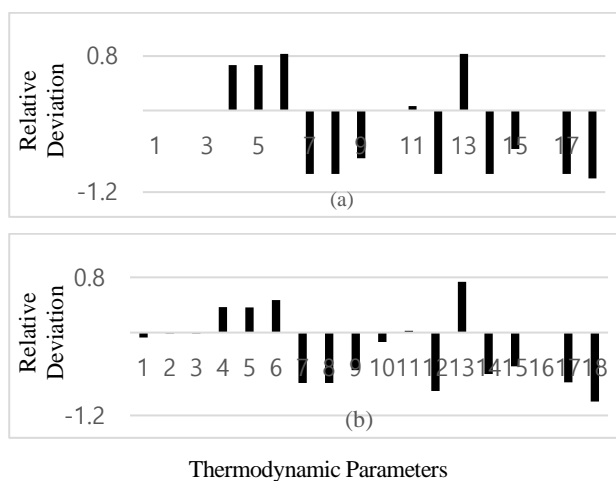


Figure 22: Normalized relative deviations under different air filters l/d and running speeds

5. Conclusion

The proposed average thermodynamic simulation model for diesel engine turbocharging and gas-changing systems is available in MATLAB/Simulink. By changing the boundary conditions and relevant model parameters, performance failures including extremely high engine room temperature, intake filter blockage, intercooler fouling at the water side, extremely high intercooler cooling water temperature, scavenging port fouling, clogged turbine nozzle, worn turbocharger bearing, and turbine exhaust passage fouling can be simulated. The relative deviations of the thermodynamic parameters under different boundary conditions and different failures are analyzed, demonstrating the inherent relationship between the thermodynamic parameters and performance failures and could be mostly free of engine running conditions. By normalizing the parameters, the influence of different boundary conditions and running conditions could be eliminated, and the performance failure diagnosis of the diesel engine under different running conditions could be realized in practice. Further research will be carried out to verify the feasibility of this method in the application of the failure detection of diesel engines on board ships.

Acknowledgement

This research work was supported by the Science & Technology Commission of Shanghai Municipality and Shanghai Engineering Research Center of Ship Intelligent Maintenance and Energy Efficiency under Grant 20DZ2252300.

Author Contributions

Conceptualization, Y. Hu; Methodology, C. Zeng and M. Wang; Software, J. Jiang; Formal Analysis, Y. Hu and C. Zeng; Investigation, M. Wang; Resources, C. Zeng; Data Curation, M. Wang; Writing-Original Draft Preparation, Y. Hu and C. Zeng; Writing-Review & Editing, Y. Hu; Visualization, M. Wang; Supervision, Y. Hu; Project Administration, Y. Hu; Funding Acquisition, Y. Hu.

References

- [1] Hu Yihuai, Accident Analysis and Safety Assessment of Marine Machinery System, Beijing, China Communications Press, 2013:94-100 (in Chinese).
- [2] D. T. Hountalas and A. D. Kouremenos, "Development and application of a fully automatic troubleshooting method for

- large marine diesel engines,” *Applied Thermal Engineering*, vol. 19, no. 3, pp. 299-324, 1999.
- [3] D. T. Hountalas, “Prediction of marine diesel engine performance under fault conditions,” *Applied Thermal Engineering*, vol. 20, no. 18, pp. 1753-1783, 2000.
- [4] N. F. Sakellariadis, S. I. Raptotasio, A. K. Antonopoulos, and *et al.*, “Development and validation of a new turbocharger simulation methodology for marine two stroke diesel engine modelling and diagnostic applications,” *Energy*, no. 91, pp. 952-966, 2015.
- [5] J. A. P. Rubio, F. Vera Garcia, and *et al.*, “Marine diesel engine failure simulator based on thermodynamic model,” *Applied Thermal Engineering*, vol. 144, pp. 982-995, 2018.
- [6] G. Theotokatos, C. Guan, H. Chen, and I. Lazakis, “Development of an extended mean value engine model for predicting the marine two-stroke engine operation at varying settings,” *Energy*, vol. 143, pp. 533-545, 2018.
- [7] N. Matulić, G. Radica, and S. Nižetić, “Engine model for onboard marine engine failure simulation,” *Journal of Thermal Analysis and Calorimetry*, vol. 141, pp. 119-130, 2020.
- [8] L. Pinfang and C. Zhenxiong, “Impact of environmental conditions on operation of main engines on ships and management strategies,” *Journal of Jimei University (Natural Science Edition)*, vol. 10, no. 1, pp. 49-52, 2005 (in Chinese).
- [9] G. Hongzhong, *Thermal Process Simulation Calculation of Turbocharged Diesel Engine*, Shanghai, Shanghai Jiaotong University Press, 1985 (in Chinese).
- [10] L. Lianxi and H. Zhiyong, and Liu Chi, “Simulation and optimization of flow resistance and noise characteristics of air cleaner,” *Automotive Engineering*, vol. 33, no. 12, pp. 1092-1097, 2011 (in Chinese).
- [11] W. Haiyan, H. Weijian, and Z. Xusheng, “Turbocharger thermodynamic model and diesel engine dynamic simulation,” *Internal Combustion Engine Engineering*, vol. 38, no. 2, pp. 128-134, 2017 (in Chinese).
- [12] G. Linfu, M. Chaocheng, and S. Xin, “Establishment, verification and simulation of steady state matching model between leaved ordinary turbocharger and engine,” *Internal Combustion Engine Engineering*, no. 3, pp. 66-68, 2003 (in Chinese).
- [13] S. Yingmei and G. Shilun, “Average model and simulation of turbocharged diesel engine,” *Diesel Engine Design and Manufacture*, no. 2, pp. 19-23, 2004 (in Chinese).
- [14] L. Ruishui, *Research on Modeling and Model Checking Methods of Average Value of Turbocharged Diesel Engine*, M. S. Thesis, Beijing University of Technology, China, 2014 (in Chinese).